Journal of Materials Chemistry C

Accepted Manuscript

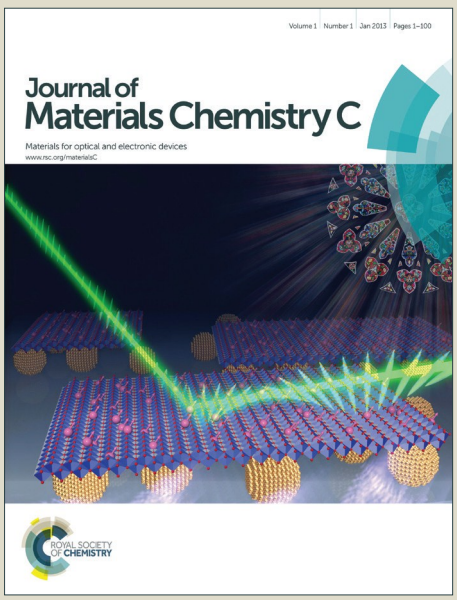

ROYAL SOCIETY OF CHEMISTRY

www.rsc.org/materialsC

Mechanical strain induced fluorescent lifetime variation in hybrid bistable $[Fe(H\text{-}trz)_2(trz)]BF_4@SiO_2@$pyrene nanoparticles.

Journal Name

RSCPublishing

ARTICLE

Electronic communication between fluorescent pyrene excimers and spin crossover complexes in nanocomposite particles

Cite this: DOI: 10.1039/x0xx00000x

Received 00th January 2012,
Accepted 00th January 2012

DOI: 10.1039/x0xx00000x

www.rsc.org/

I. Suleimanov,[a,b] O. Kraieva,[a,c] J. Sánchez Costa,[a] I. O. Fritsky,[b] G. Molnár,[a] L. Salmon*[a] and A. Bousseksou*[a]

Bistable [Fe(H-trz)2(trz)]BF4 core and silica shell hybrid nanoparticles with different sizes between 50 – 150 nm were grafted with a pyrene-derivative fluorophore. The fluorescent composites exhibited both monomer and excimer luminescence (with controllable ratio), whilst their spin transition properties remained unaltered. When switching the particles from the diamagnetic to the paramagnetic state the excimer lifetime and luminescence intensity increased and the emission spectra was redshifted, while the monomer emission exhibited negligible spin-state dependence. The strong coupling of the pyrene excimers with the spin-state of the ferrous ions was shown to occur via a non-radiative mechanism, brought about, to a large extent, by the spin transition induced mechanical strain.

Introduction

Certain $3d^4$ – $3d^7$ transition metal ion complexes are known to exhibit one of the most fascinating molecular bistability phenomena called spin crossover (SCO).[1,2] The switching between the low spin (LS) and high spin (HS) electronic states can be provoked by different external perturbations such as temperature change, light irradiation, application of pressure or high magnetic fields and host-guest interactions. Due to the drastic changes of the physical properties (optical absorption, magnetic susceptibility, density, etc), which accompany the spin state switching, these materials have attracted considerable attention for applications in sensor, display and memory devices.[3]

Recently, a significant interest have arisen in the synthesis of materials containing SCO as well as fluorescent moieties displaying potentially very interesting synergy between these two electronic phenomena at the molecular or supramolecular levels.[4] The main appeal of these hybrid materials is related to the fact that fluorescence intensity is a sensitive probe of the spin-state of the system and can provide high signal contrast and sensitivity, especially in temporally or spatially resolved measurements. Besides, the SCO phenomenon may allow for the switching and modulation of the luminescent signal as well as for detecting physicochemical changes in the environment of the SCO centre. All these benefits could be used for the development of photonic switches[5], thermometers[6] or gas sensors[7]. There is also a fundamental interest of studying energy transfer mechanisms between fluorophores and transition metal complexes in their different spin states.[8]
Nevertheless, bringing together the SCO and fluorophore moieties within a functional material is still a great challenge. Until now, there are some examples of luminescent SCO materials containing a luminescent moiety either as a part of the SCO compound itself (ligands, counterions) or introduced as a dopant at some position of the SCO host lattice. The first strategy has led so far only to a rather limited success[9] mainly because of the risk to lose one or both properties when combining the luminophore and the SCO metal within the same entity. This problem is largely reduced in the case of the doping approach, especially for low (< few %) dopant concentrations. The doping strategy was successfully implemented using different organic luminophores and SCO complexes both in bulk and nanoscale materials.[6,10] In most cases the luminescence intensity variation in response to the spin state switching was interpreted as a consequence of the efficient spectral overlap between the fluorophore emission and the absorption of the SCO complex in a given spin state (usually the LS state for ferrous complexes) - leading to enhanced excited state energy transfer from the luminophore to the complex in that spin state, i.e. to a decrease of the luminescence intensity. Depending on the spatial proximity of the luminescent and SCO centres this energy transfer can be either radiative or resonant (e.g. Förster type), but the available experimental data usually did not allow to discuss the microscopic details of the quenching mechanism.

In this paper we propose a novel approach for luminescence modulation by SCO, which is based on the spatially-sensitive features of the excimer luminescence of pyrene. Pyrene is a well-known polyaromatic fluorophore with remarkable photophysical properties.[11] Of particular interest for us is the pyrene excimer emission, which occurs when a ground state and an excited state pyrene moiety is in close proximity (~10 Å) one to another. This gives rise to the excited dimer (i.e. excimer) formation. The excimer/monomer fluorescence intensity ratio is an indicator of the spatial proximity and

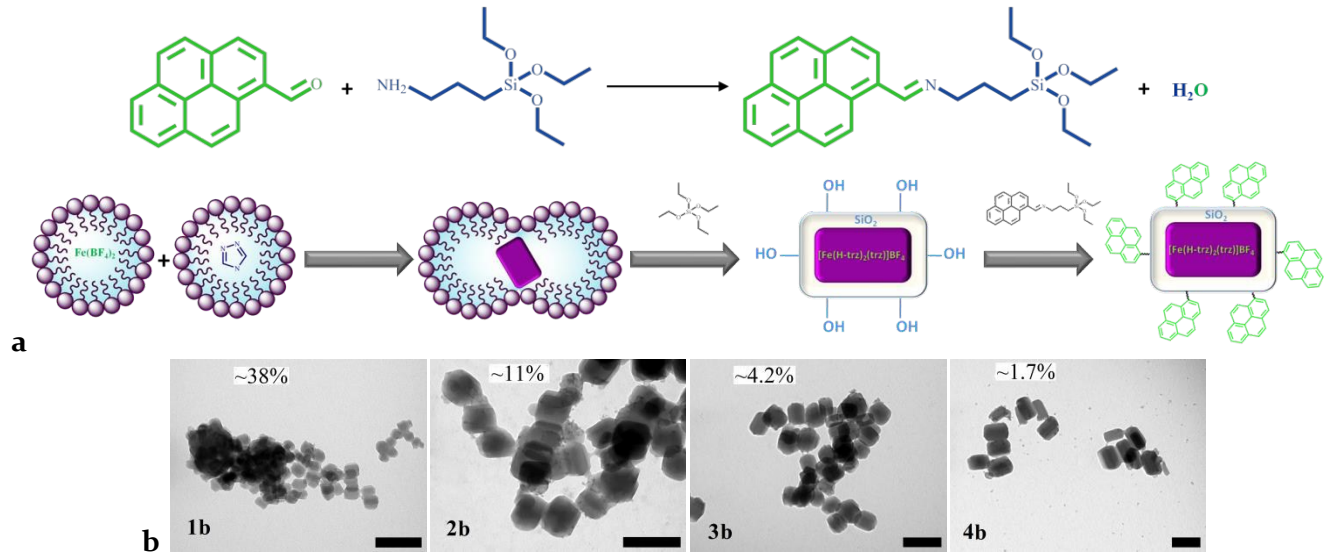

Fig 1. (a) Synthetic route for pyrene-grafted $[Fe(H\text{-}trz)_2(trz)]BF_4@SiO_2$ core-shell particles, (b) representative TEM images of samples **1b** – **4b**. The fluorophore content (mass %) is indicated for each nanocomposite. Scale bares are 200 nm.

orientation between two pyrene moieties (either free or covalently attached to other molecules of interest). This approach has been widely used in various fields of science from organic electronics[12] to biology[13,14] as a sensitive probe to study structure, conformation, intra- or intermolecular interactions and their dynamics as well as mechanical strain in different samples. Owing to the strong electron-lattice coupling, the spin transition from the HS to the LS state involves a very significant lattice contraction (typically 1 – 10 %). It is thus tempting to use the spatial sensitivity of excimer luminescence of pyrene to probe the spin transition. This idea can be implemented in different ways. González-Prieto *et al.*[15] designed SCO complexes with ligands functionalized with pyrene. Strong intermolecular π-π stacking led to both monomer and excimer pyrene luminescence in the bulk solid complexes, but the temperature dependence of these emissions reflected mainly the ordinary thermal extinction and no clear correlation with the spin state of the complexes could be established. The approach we adopted here is different: it is based on the hierarchical assembly of the SCO and pyrene entities. We elaborated $[Fe(H\text{-}trz)_2(trz)]BF_4$ based $SCO@SiO_2$ core-shell nanoparticles (H-trz = 1,2,4-triazole and trz = 1,2,4-triazolato), which we surface grafted with a pyrene containing fluorophore. This SCO complex was chosen because of its robust and abrupt spin transition associated with a wide thermal hysteresis even in nanoparticles,[16,17] and a huge volume change of 11.5 %, while the overall architecture was inspired by the work of Titos-Padilla et al.[10d] These authors reported on the synthesis of $[Fe_xZn_{1-x}(H\text{-}trz)_2(trz)]BF_4$ nanoparticles embedded within a SiO_2 shell and decorated by 3-(dansylamido)-propyl-trimethoxysilane fluorophores. Their approach can be considered also as a form of doping luminophores into the SCO material, the essential difference being that the luminophore is confined to the surface of the particles. This latter property is what we aimed to use in order to achieve pyrene excimer luminescence.

Results and analysis

Luminescent SCO nanopartilces (NPs) were prepared using a two-step method (Fig. 1a). In the first step SCO NPs with a thin outer silica shell were prepared using similar reverse microemulsion technique as described previously.[18] The triethoxysilane functionalized pyrene molecule[19] (Py-CH=N-PTS) was then grafted on the particle surface. Platelet-like particles with length (width) between ca. 60 - 150 nm (40 – 90 nm) were obtained by varying the cyclohexane quantity used in the microemulsion preparation. For a given particle size the quantity of grafted fluorophore molecules and thus the monomer/excimer fluorescence ratio can be adjusted to some extent, but (virtually) pure monomer and excimer emissions could be obtained only for different sized particles.

Overall four samples (**1b** – **4b**) with decreasing fluorophore quantities (38, 11, 4.2, 1.7 % mass, determined by elemental analyses) have been prepared (Fig. 1b), see also the Supporting Information, (SI) for color, FTIR spectra, transmission electron microscopy (TEM) of each sample. Room temperature absorption, excitation and emission spectra of the luminophore in a diluted chloroform solution are shown in Fig. 2a. Both the absorption and emission spectra are similar to that of unsubstituted pyrene, but with the expected bathochromic shift caused by the substituent.[11,20] The transition between the lowest vibrational levels of the ground S_0 and the first excited electronic state S_1 (the so-called 0-0 transition) is probably situated around 440 nm in the absorption spectrum with a small extinction coefficient. Transitions to higher energy excited states (S_0-S_2, S_0-S_3 and S_0-S_4) are clearly observed around 348, 278 and 245 nm, respectively and even their vibronic fine structure is resolved. Despite the low absorption coefficient of the 0-0 transition, photoluminescence still can be excited in the visible region using blue light. In other cases, the S_0-S_2 transition is preferable for excitation for its relatively high molar absorption coefficient. In the emission spectrum there are two well separated bands: the monomer emission in the 378 - 417 nm range with ill-resolved vibronic fine structure and the broad excimer emission centered at 480 nm. Emission spectra of powder samples of **1b** – **4b** were recorded at room temperature with an excitation wavelength of 348 nm (Fig. 2b).

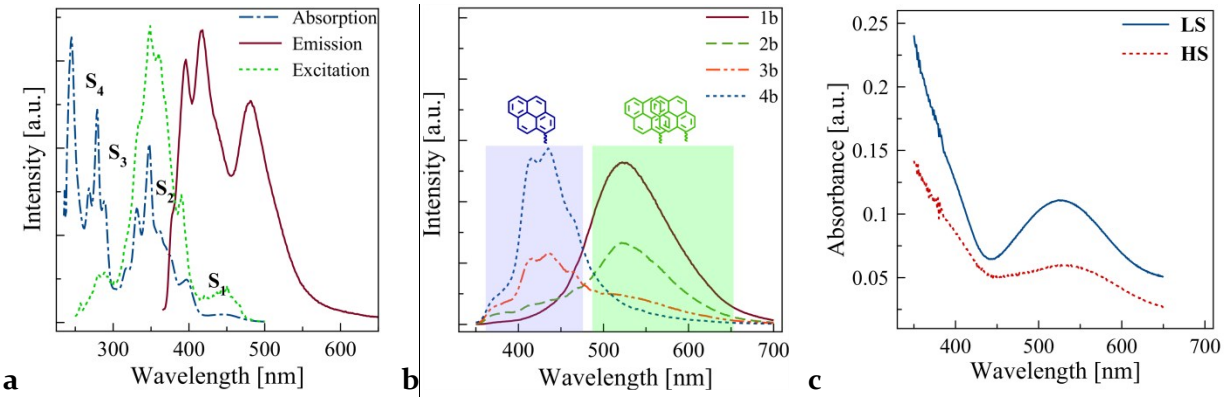

Fig. 2. (a) Room temperature absorption, luminescence excitation (λemission = 480 nm) and emission (λexcitation = 348 nm) spectra of the luminophore in chloroform (10-3 mol·L-1), (b) emission spectra (λexc = 348 nm, T = 293 K) of samples 1b – 4b in the solid state, (c) absorption spectra of the SCO complex in the LS (293 K) and HS (400 K) states.

These spectra are red-shifted and broadened when compared to that of the free fluorophore. These changes are more pronounced for the excimer emission band, which is shifted to 520 nm and its full width at half-maximum increases from 65 to 110 nm. The excimer to monomer ratio changes drastically from sample to sample. For **1b** (**4b**), with the highest (lowest) fluorophore quantity, the excimer (monomer) band dominates the emission spectrum, while for **2b** and **3b** both emissions are clearly discernible with different ratios, reflecting the different quantity of the grafted pyrene species. It is interesting to correlate the luminescence spectra of our samples with the absorption spectra of $[Fe(H\text{-}trz)_2(trz)]BF_4$ (Fig. 2c).

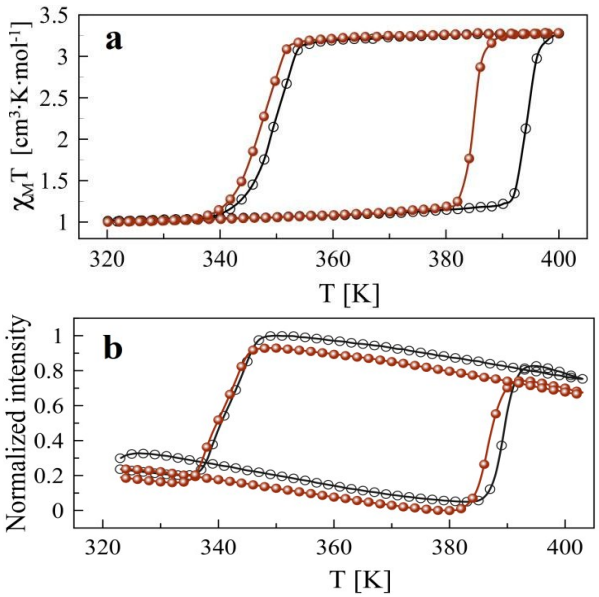

Fig. 3. Molar magnetic susceptibility vs. temperature product (a) and normalized excimer luminescence intensity recorded at 550 nm (b) as a function of the temperature for sample **1b** for two successive thermal cycles (empty /full circles: first/second cycle).

In the LS state of the complex one can observe the $^1A \rightarrow {}^1T$ absorption centered at 530 nm, which perfectly overlaps with the excimer emission band. Switching from the LS to the HS state leads to the (reversible) bleaching of the absorption band at 530 nm and a weak, broad absorption appears in the near infrared range (not shown), which can be assigned to the $^5T \rightarrow {}^5E$ transition. It is worth noting also that the tail of the charge transfer band(s) below ca. 450 nm is more intense in the LS state. Residual absorbance in the HS state is ascribed to a residual LS fraction due to the temperature inhomogeneity across the sample during the measurement at high temperature (400 K).

Variable temperature magnetic susceptibility measurements for samples **1b** – **4b** reveal the well-known spin transition of $[Fe(H\text{-}trz)_2(trz)]BF_4$. For each sample the transition temperature for the first heating mode is somewhat higher when compared to the second cycle (due probably to solvent release), but further cycling does not influence significantly the transition temperatures. For **1b** the LS to HS (HS to LS) transition occurs in an abrupt manner around 384 K (347 K) defining thus a broad hysteresis with 37 K width (Fig. 3a). The other samples exhibit similar behavior (see the SI for more details). Normalized fluorescence intensity recorded at 550 nm is shown in Fig. 3b as function of temperature for sample **1b**. On heating to ca. 380 K the luminescence exhibits a slight linear decrease, which corresponds to the thermal population of non-emitting states (thermal quenching). Around the LS to HS transition temperature the luminescence intensity increases in an abrupt manner. In the cooling mode the luminescence intensity first increases, then around 345 K it exhibits an abrupt drop. The thermal hysteresis loop observed in the fluorescence and magnetic measurements are in good agreement. It should be noted that long exposition to light leads to photobleaching, which explains the slightly decreased luminescence intensity during the second thermal cycle. (The photobleaching rate depends obviously on the duration and the spectral intensity of the light exposure.) Overall, the response of the other samples was found fairly similar (see the SI). While the absolute excimer fluorescence intensity increases monotonously with increasing luminophore quantity, the fluorescence intensity change during the spin transition exhibits an inverse tendency: the luminescence intensity changes by ca. 45 % for samples **3b** and **4b**, while only 25-30 % modulation is obtained for samples **1b** and **2b**. These differences might be related to self-quenching

phenomena in the concentrated samples. Incidentally, it may be worth noting that within the spin transition temperature range the variation of luminescence intensity can be as high as 5 %/K. This sensitivity is about two orders of magnitude higher than that of the thermal quenching and similar to the best reported luminescent thermometers providing thus prospects for the use of luminescent SCO hybrids for thermometry purposes.[6,22]

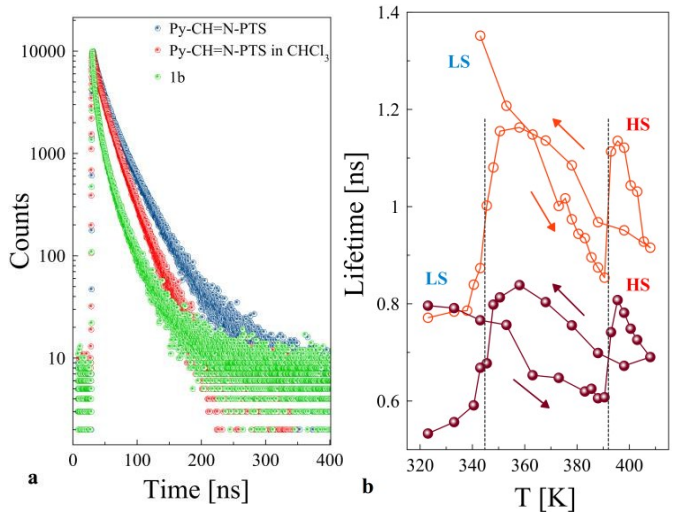

Fig. 4. (a) Luminescence decay curves (λexcitation = 303 nm, λemission = 550 nm, T = 293 K) of the pure and the diluted (in chloroform) luminophore and that of sample **1b** (in this order from top to down). (b) Temperature dependence of the (mean) excimer lifetime for sample **1b** across two thermal cycles (empty/full circles: first/second cycle). The dotted vertical lines indicate the spin transition temperatures.

Room temperature excimer luminescence decay curves of the solid-state fluorophore and its chloroform solution (10^{-3} mol·L^{-1}) are shown in Fig. 4a. The raw data were fitted with a multi-exponential decay and the average excimer lifetimes were calculated as[23]:

$$F(t) = A + B_1 \exp\left(\frac{-t}{T_1}\right) + B_2 \exp\left(\frac{-t}{T_2}\right) + B_3 \exp\left(\frac{-t}{T_3}\right)$$

$$\tau_{ave} = B_1T_1 + B_2T_2 + B_3T_3$$

The average excimer lifetimes are 21 ns and 17 ns for the pure and diluted free luminophore, respectively. The latter value is significantly smaller than those reported for unsubstituted pyrene in various solvents (43 - 65 ns).[11] This may be related to the presence of oxygen (air) in our measurements.[21] The average room temperature excimer lifetime in sample **1b** is only 7 ns (Fig. 4a), while for samples **2b** – **4b** it further decreases to 3 - 4 ns, respectively (see the SI). Shorter lifetimes which were found for samples **1b** – **4b** indicate more efficient nonradiative energy transfer pathways. Similar results have been reported very recently by Herrera *at al.* using a dansyl-derivate fluorophore.[24] Our main interest here, however, is the investigation of the luminescence lifetime changes during the spin transition, which has never been reported to our best knowledge. The average excimer lifetime was determined for sample **1b** both in the heating and cooling modes with a step of 2.5 K around the spin transition regions, while steps of 15 K were used elsewhere. To eliminate traces of solvents the sample was first heated to 403 K and cooled to 323 K. The temperature dependence of τ_{ave} for two consecutive thermal cycles is shown in Fig. 4b. Unfortunately this experiment involves a prolonged exposure to relatively strong

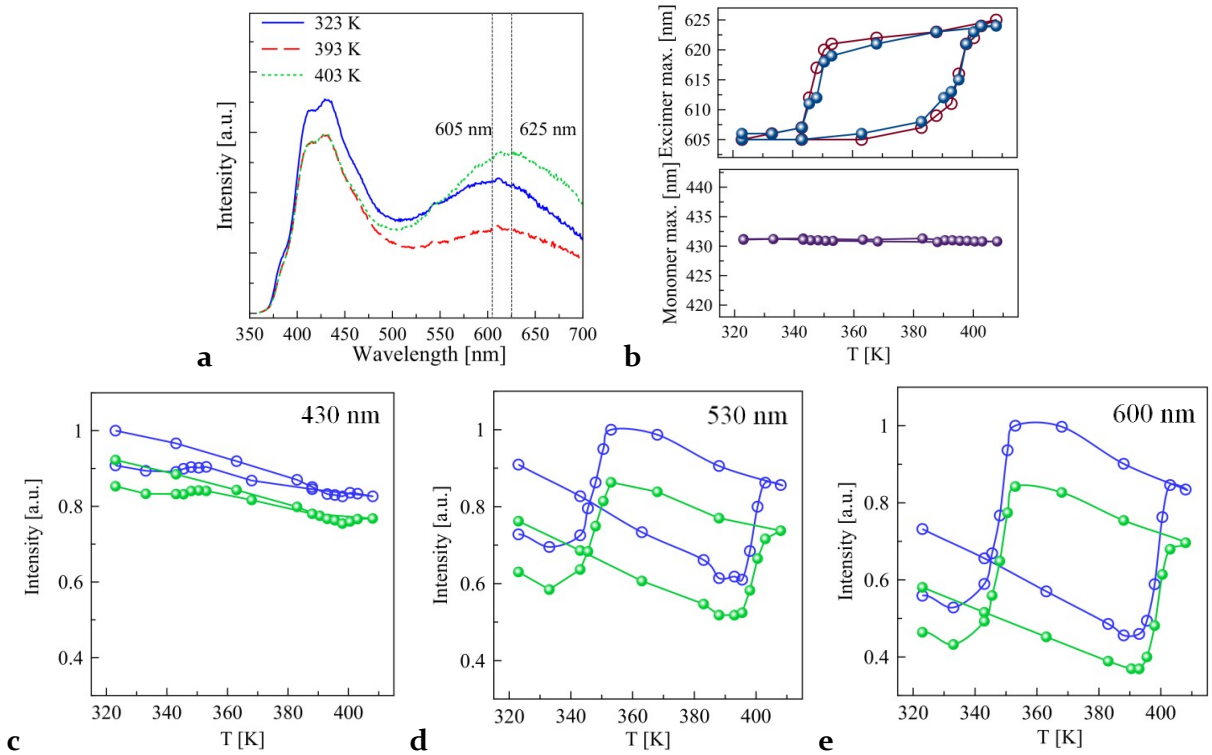

Fig. 5. (a) Luminescence emission spectra (λexcitation = 348 nm) of sample **3b** at selected temperatures in the heating mode. Temperature dependence of the excimer and monomer luminescence peak wavelengths (b) and luminophore intensities at different wavelengths (c-e) for sample **3b** across two thermal cycles (empty/full circles: first/second cycle).

laser excitation and the photobleaching leads to a continuous drift of the average lifetime values. Nevertheless, we can draw two clear-cut conclusions from these data. First, as expected the excimer lifetime decreases with increasing temperature. This finding is also in good agreement with the thermal decrease of luminescence intensity reported in Fig. 3b and can beexplained by the thermal activation of non-radiative relaxation channels. More interesting is the observation of the excimer lifetime increase when switching the spin-state of the particles from the LS to the HS state. For the first thermal cycle the excimer lifetime change is 0.28 ns (heating mode) and 0.38 ns (cooling mode), while for the second cycle these values are 0.21 and 0.23 ns, respectively. The luminescence intensity increase when going from the LS to the HS state may be explained by an energy transfer mechanism by considering the very significant spectral overlap between the LS absorption (Fig. 2c) and the excimer emission (Fig. 2b) bands. This energy transfer may occur either by reabsorption of emitted photons (radiative transfer) or by a resonant (radiationless) transfer mechanism. The decrease of the luminescence lifetime in the LS state supports the latter scenario, since a radiative energy transfer process is not expected to influence the lifetime of the emitting state. However, for a radiationless process the energy transfer rate depends strongly on the donor – acceptor distance as well as on the extinction coefficient of the acceptor. In our case the luminescent and SCO centers are separated by a silica shell of a few nanometers thickness[18] and the absorption of the SCO centers corresponds to a Laporte forbidden weak ligand-field transition. These two facts cast doubt on the possibility of an efficient resonant energy transfer process in our nanocomposites. To better understand the mechanistic details of the spin-state sensitivity of the excimer luminescence we have recorded thus the temperature dependent emission spectrum of sample **3b**, which exhibits both significant excimer and monomer emission intensities. To eliminate traces of solvents the sample was first heated to 403 K and cooled to 323 K which resulted in a further red-shift (from 525 nm to 605 nm) and broadening of the excimer emission peak. As shown in Figure 5 the excimer band intensity as well as peak wavelength depends strongly on the spin state of the system. On the other hand, the monomer peak wavelength remains virtually unchanged and its intensity shows only temperature dependence - it remains nearly unaltered by the spin transition. Even if the spectral overlap of the excimer luminescence with the LS absorption bands is higher the monomer emission exhibits also some overlap. One would expect therefore that both emissions were modulated if resonant energy transfer occurs in the system. Indeed, the comparison of Fig. 5c – 5e with Fig. 2c reveals a lack of spectral correlation of the luminescence intensity changes with the absorbance changes in the SCO complex. In addition the redshift of the excimer luminescence in the HS state is also difficult to explain with an energy transfer mechanism mediated by the spectral overlaps. For these reasons it seems more plausible that the observed spin-state sensitivity of the excimer luminescence is related to another mechanism. As the spin transition in $[Fe(H\text{-}trz)_2(trz)]BF_4$ involves a very significant unit-cell volume change ($\Delta V/V \sim 11.5$ %)[25] it may produce some spatial distortions on pyrene-pyrene excited dimer formation. Such mechanically induced disturbing of the excimer formation in pyrene-based liquid crystals and polymers was reported to lead to the excimer emission shift and intensity variation.[26] We suggest therefore that the mechanical strain is the key factor in the variation of the excimer luminescence properties upon the spin transition phenomenon in our system. Further studies with different luminophores and particle morphologies will be needed to precisely quantify the different contributions to the electronic communication between excimers and SCO entities.

Experimental

Materials and methods

All chemicals and solvents were obtained from Sigma Aldrich or Alfa-Aesar and used without any further purification. Transmission electron microscopy images were acquired with a JEOL JEM-1011 (100 kV) instrument. CHN elemental analysis was done using a Flash EA1112 (Thermo Finnigan) apparatus. Infrared absorption spectra were recorded with a Perkin Elmer Spectrum 100 spectrometer in ATR mode between 650 and 4000 cm−1 with 2 cm−1 resolution. Variable temperature luminescence excitation and emission spectra were recorded using a Fluoromax-4 (Horiba) spectrofluorimeter and a THMS600 liquid nitrogen cryostat (Linkam Scientific Instruments). Fluorescence data were corrected for the instrumental response as implemented in the software. UV-vis absorption spectra were recorded with a Cary-50 (Varian) spectrophotometer using 1 cm quartz cuvette. Variable temperature diffuse reflectance spectra were recorded with a Lambda 35 UV/Vis spectrophotometer equipped with a Labsphere RSA-PE-20 integrating sphere and a Peltier module. Variable temperature magnetic data for the powdered samples were collected with a Quantum Design MPMS2 magnetometer under a magnetic field of 1 T at a rate of 2 K/min. Magnetic susceptibility data were corrected for the diamagnetic contributions. Variable temperature fluorescence intensity measurements have been carried out using an Olympus BX51 microscope equipped with an iKon-M DU934N- BV (Andor Technology) charge-coupled device detector. An objective with a ×5 magnification (numerical aperture, NA = 0.1) was used. A dichroic mirror (cutting edge at 510 nm) was used to separate the excitation and collected light beams. Two band-pass filters were used, one for the excitation, centered at 450 nm (full width at half maximum, FWHM = 45 nm) and another one for the emitted light at 550 nm (FWHM = 50 nm). Pressed powdered samples were heated and cooled at a rate of 2 K/min by means of the THMS-600 cryostat. Variable temperature luminescence lifetime measurements were performed using the time-correlated single photon counting (TCSPC) technique using a DeltaFlex (Horiba) instrument equipped with a 303 nm electroluminescent diode (pulse duration 1.2 ns) and the THMS-600 cryostat. Fittings and lifetime calculations were performed using DAS6 fluorescence decay analysis software.

Synthetic procedures

Fluorophore synthesis. Py-CH=N-PTS has been synthesized as follows: 0.5 g (2.17 mmol) of 1-pyrenecarboxaldehyde was

dissolved in 50 ml of methanol under heating. A solution of 0.48 g (2.17 mmol) 3-aminopropyltriethoxysilane in 2 ml of methanol was then added. This mixture was stirred at 50°C for approximately 24 hours. The final product in the form of yellow oil was obtained by evaporation of the solvent using rotary evaporator. 1HNMR (400 MHz, CDCl3, δ, ppm): 9.32 (1H, s), 8.94 (1H, d, J = 9.16 Hz), 8.55 (1H, d, J = 7.99 Hz), 8.25-8.02 (7H, m), 3.89 (6H, q, J = 7.02 Hz), 3.63 (2H, t, J = 2.55 Hz), 2.02 (2H, dt, J = 8.16 Hz, J = 2.55 Hz), 1.28 (9H, t, J = 7.02 Hz), 0.84 (2H, t, J = 8.16 Hz). Elemental analysis: Calc. C: 72.02; H: 7.21; N: 3.23. Observed: C: 71.34; H: 6.92; N, 3.17.

Luminescent nanoparticle synthesis. The particles were synthesized in two steps. The SCO@SiO_2 particles were prepared in the first step. Sample **1a**: an aqueous solution of $Fe(BF_4)_2$ $6H_2O$ (422 mg, 1.25 mmol in 1 mL H_2O) was added dropwise to a mixture of 0.1 mL of tetraethylorthosilicate (TEOS), 3.6 mL of Triton X-100, 3.6 mL of 1-hexanol and 7.5 mL of cyclohexane. The identical microemulsion was prepared with a solution of H-trz (262 mg, 3.75 mmol in 1 mL H_2O). These two microemulsions were mixed together and left to stir for 24h. The obtained nanoparticles were separated and washed three times with ethanol. **2a**-**4a** were prepared using the same method, but with different reagent quantities (see Table S1). The second step consists in fluorophore grafting on the NPs surface. Thanks to the triethoxysilane group of the fluorophore it can be chemically bonded to the SiO_2 outer shell. Sample 1b: 100 mg of 1a was dispersed in 20 ml of ethanol and 50 mg of Py-CH=N-PTS was added. The obtained mixture was refluxed for 3 hours while stirring. Finally, the NPs were separated by centrifugation and washed at least five times with ethanol to remove the unattached pyrene. **2b**-**4b** were prepared using the same method, but with different fluorophore quantities (see Table S2).

Conclusions

In summary, we synthesized new pyrene-functionalized spin crossover nanocomposites displaying both excimer and monomer pyrene luminescence. It was shown that the spin-state switching influences, in a perfectly reversible manner, the intensity, the wavelength as well as the excited state lifetime of pyrene excimer luminescence, while the monomer emission remains nearly unaffected. Owing to the large thermal hysteresis and the abruptness of the spin transition these phenomena could be easily distinguished from ordinary thermal quenching and photobleaching effects. The spin-state sensitivity of the excimer emission was attributed to pyrene-pyrene distance and orientation changes driven by the spontaneous strain accompanying the spin transition – even if contributions from energy transfer processes could not be excluded. This new concept of hybrid luminescent SCO materials based on the spatial sensitivity of excimer luminescence provides a novel example for the quickly growing interest of using the mechanical strain of SCO materials in hybrid systems, such as in actuator devices[27,28], magnetostrictive systems[28] and switchable electronic devices.[30,31]

Acknowledgements

This work was financially supported by the project ANR-13-BS07-0020-01. I.S. thanks the French Embassy in Ukraine for financial support. J.S.C. thanks the Marie-Curie research program (NanoSCOpe 328078). The research have been performed within the framework of the GDRI (Groupement Franco-Ukrainien en Chimie Moléculaire).

Notes and references

[a] Laboratoire de Chimie de Coordination, CNRS & Université de Toulouse (INPT, UPS), 31077 Toulouse, France. E-mails: azzedine.bousseksou@lcc-toulouse.fr; lionel.salmon@lcc-toulouse.fr
[b] Department of Chemistry, Taras Shevchenko National University of Kyiv, 01601 Kyiv, Ukraine
[c] Kyiv Polytechnic Institute, National Technical University of Ukraine, 03056 Kyiv, Ukraine

† Electronic Supplementary Information (ESI) available: synthesis details, sample color, elemental analysis, particle size distribution from TEM, magnetic and luminescence data for **2b** – **4b**. See DOI: 10.1039/b000000x/

1 P. Gütlich and H. A. Goodwin, Spin Crossover in Transition Metal Compounds: Topics in Current Chemistry, Springer, Berlin, 2004.
2 P. Gütlich, A. Hauser, H. Spiering, *Angew. Chem. Int. Ed*. 1994, **33**, 2024.
3 A. Bousseksou, G. Molnár, L. Salmon, W. Nicolazzi, *Chem. Soc. Rev*. 2011, **40**, 3313.
4 H. J. Shepherd, C. M. Quintero, G. Molnár, L. Salmon, A. Bousseksou, In Spin-Crossover Materials; Ed. M. A. Halcrow, John Wiley & Sons Ltd: Oxford, UK, 2013, pp. 347–373.
5 M. Matsuda, H. Isozaki, H. Tajima, *Chem. Lett*. 2008, **37**, 374.
6 L. Salmon, G. Molnár, D. Zitouni, C. Quintero, C. Bergaud, J.-C. Micheau, A. Bousseksou, *J. Mater. Chem*. 2010, **20**, 5499.
7 G. Molnár, I. A. Gural'skyi, L. Salmon, W. Nicolazzi, C. Quintero, A. Akou, K. Abdul-Kader, G. Félix, T. Mahfoud, C. Bergaud, C. Bartual-Murgui, C. Thibault, C. Vieu, A. Bousseksou, Proceedings of SPIE 2012; Vol. 8425, p 842513.
8 C. Edder, C. Piguet, J.-C. G. Bünzli, G. Hopfgartner, *Chem. Eur. J*. 2001, **7**, 3014.
9 (a) M. Engeser, L. Fabbrizzi, M. Licchelli, D. Sacchi, *Chem. Commun*. 1999, 1191. (b) M. Hasegawa, F. Renz, T. Hara, Y. Kikuchi, Y. Fukuda, J. Okubo, T. Hoshi, W. Linert, *Chem. Phys*. 2002, **277**, 21. (c) H. Matsukizono, K. Kuroiwa, N. Kimizuka, *Chem. Lett*. 2008, **37**, 446. (d) A. Santoro, L. J. Kershaw Cook, R. Kulmaczewski, S. A. Barrett, O. Cespedes, M. A. Halcrow, *Inorg. Chem*. 2015, **54**, 682. (e) Y. Garcia, F. Robert, A. D. Naik, G. Zhou, B. Tinant, K. Robeyns, S. Michotte, L. Piraux, *J. Am. Chem. Soc*. 2011, **133**, 15850.
10 (a) C. A. Tovee, C. A. Kilner, J. A. Thomas, M. A. Halcrow, *CrystEngComm* 2009, **11**, 2069. (b) M. Matsuda, H. Isozaki, H. Tajima, *Thin Solid Films* 2008, **517**, 1465. (c) C. M. Quintero, I. A. Gural'skiy, L. Salmon, G. Molnár, C. Bergaud, A. Bousseksou, *J. Mater. Chem*. 2012, **22**, 3745. (d) S. Titos-Padilla, J. M. Herrera, X.-W. Chen, J. J. Delgado, E. Colacio, *Angew. Chem. Int. Ed*. 2011, **50**, 3290. (e) I. A. Gural'skiy, C. M. Quintero, K. Abdul-Kader, M. Lopes, C. Bartual-Murgui, L. Salmon, P. Zhao, G. Molnár, D. Astruc, A. Bousseksou, *J. Nanophotonics* 2012, **6**, 063517. (f) C. Quintero,

G. Molnár, L. Salmon, A. Tokarev, C. Bergaud, A. Bousseksou, In 2010 16th International Workshop on Thermal Investigations of ICs and Systems (THERMINIC); 2010; pp 1–5.
11 J. B. Birks, Photophysics of Aromatic Molecules; John Wiley & Sons Ltd: London, New York, 1970.
12 T. M. Figueira-Duarte, K. Müllen, *Chem. Rev*. 2011, **111**, 7260.
13 G. Bains, A. B. Patel, V. Narayanaswami, *Molecules* 2011, **16**, 7909.
14 G. K. Bains, S. H. Kim, E. J. Sorin, V. Narayanaswami, *Biochemistry* 2012, **51**, 6207.
15 R. González-Prieto, B. Fleury, F. Schramm, G. Zoppellaro, R. Chandrasekar, O. Fuhr, S. Lebedkin, M. Kappes, M. Ruben, *Dalton Trans.* 2011, **40**, 7564.
16 J. Kröber, E. Codjovi, O. Kahn, F. Grolière, C. Jay, *J. Am. Chem. Soc.* 1993, **115**, 9810.
17 J. R. Galán-Mascarós, E. Coronado, A. Forment-Aliaga, M. Monrabal-Capilla, E. Pinilla-Cienfuegos, M. Ceolin, *Inorg. Chem*. 2010, **49**, 5706.
18 I. Suleimanov, J. Sánchez Costa, G. Molnár, L. Salmon, A. Bousseksou, *Chem Commun* 2014, **50**, 13015.
19 Y. Matsuo, T. Fukutsuka, Y. Sugie, *Chem. Lett*. 2006, **35**, 530.
20 J. Duhamel, *Polymers* 2012, **4**, 211.
21 D. S. Karpovich, G. J Blanchard, *J. Phys. Chem*. 1995, **99**, 3951.
22 C. D. S. Brites, P. P. Lima, N. J. O Silva, A. Millán, V. S. Amaral, F. Palacio, L. D. Carlos, *Nanoscale* 2012, **4**, 4799.
23 J. R. Lakowicz, Principles of Fluorescence Spectroscopy, 3rd Edition, Springer Science + Business Media, New York, 2006.
24 J. M. Herrera, S. Titos-Padilla, S. Pope, I. Berlanga, F. Zamora, J. J. Delgado, K. Kamenev, X. Wang, A. Prescimone, E. K. Brechin, E. Colacio, *J. Mater. Chem. C* 2015, DOI: 10.1039/C5TC00685F.
25 A. Grosjean, P. Négrier, P. Bordet, C. Etrillard, D. Mondieig, S. Pechev, E. Lebraud, J.-F. Létard, P. Guionneau, *Eur. J. Inorg. Chem.* 2013, **2013**, 796.
26 (a) Y. Sagara, T. Kato, *Angew. Chem. Int. Ed*. 2008, **47**, 5175. (b) N. A. A. Rossi, E. J. Duplock, J. Meegan, D. R. T. Roberts, J. J.Murphy, M. Patel, S. J. Holder, *J. Mater. Chem*. 2009, **19**, 7674.
27 H. J. Shepherd, I. A. Gural'skiy, C. M. Quintero, S. Tricard, L. Salmon, G. Molnár, A. Bousseksou, *Nat. Commun*. 2013, **4**, 2607
28 I. A. Gural'skiy, C. M. Quintero, J. S. Costa, P. Demont, G. Molnár, L. Salmon, H. J. Shepherd, A. Bousseksou, *J. Mater. Chem. C* 2014, **2**, 2949.
29 C. R. Gros, M. K. Peprah, B. D. Hosterman, T. V. Brinzari, P. A. Quintero, M. Sendova, M. W. Meisel, D. R. Talham, *J. Am. Chem. Soc*. 2014, **136**, 9846.
30 Y.-S Koo, J. R. Galán-Mascarós, *Adv. Mater*. 2014, **26**, 6785.
31 Y.-C. Chen, Y. Meng, Z.-P. Ni, M.-L. Tong, *J. Mater. Chem. C* 2015, **3**, 945.